Nuclear Engineering and Design 431 (2025) 113722

Contents lists available at ScienceDirect

Nuclear Engineering and Design

journal homepage: www.elsevier.com/locate/nucengdes

Validation process against late phase conditions of the passive autocatalytic recombiner simulation code PARUPM as a standalone tool using experimental data from REKO-3 and THAI facilities

Araceli Dominguez-Bugarin [a,*], Ernst-Arndt Reinecke [b], Gonzalo Jiménez [a], Miguel Ángel Jiménez [a,c], Sanjeev Gupta [d]

[a] Universidad Politécnica de Madrid, ETSI Industriales, José Gutiérrez Abascal, 2, 28006 Madrid, Spain
[b] Forschungszentrum Jülich GmbH, Wilhelm-Johnen-Straße, 52425 Jülich, Germany
[c] Consejo de Seguridad Nuclear, C/ Pedro Justo Dorado Dellmans, 11, 28040 Madrid, Spain
[d] Becker Technologies GmbH, Rahmannstraße 11, 65760 Eschborn, Germany

ARTICLE INFO

Keywords:
PARs
Hydrogen risk
Severe accident
THAI
REKO-3

ABSTRACT

In case of a nuclear accident with core damage in a light water reactor, the oxidation of the fuel cladding and other materials could lead to the release of combustible gases (H_2 and CO) to the containment building. To mitigate the potential risk of combustion of these gases, passive autocatalytic recombiners (PARs) have been installed in numerous nuclear reactors in Europe and worldwide. PARs recombine H_2 and CO with O_2 producing H_2O and CO_2, respectively, without an open flame.

PARUPM is a code that simulates the behaviour of PARs using a physicochemical model approach. In the framework of the AMHYCO project (EU-funded Horizon 2020 project), which seeks to advance the understanding and simulation capabilities to support the combustion risk management in severe accidents, the code has been extensively enhanced and developed to simulate PAR operation with $H_2/CO/O_2$/steam mixtures. Alongside these new capabilities, the code needed a new validation process.

In this paper, the process of validation of PARUPM as a standalone code is described. The validation for steady state conditions was achieved through comparison with REKO-3 experimental data while the transient conditions were compared with results obtained with the THAI test facility. A thorough analysis of the code capabilities was performed by comparing the numerical results with experimental data for a broad series of conditions, namely: a range of different input gas temperatures and concentrations, oxygen starvation, CO poisoning, etc.

1. Introduction

Hydrogen and carbon monoxide are both potentially hazardous combustible gases, that are produced during severe accidents in nuclear power plants. After mixing with air, they could pose a threat to containment integrity in case of deflagration or –particularly- detonation. To address this risk, passive auto-catalytic recombiners (PARs) have been widely installed within containment buildings in Europe (ENSREG, 2012) and worldwide (NEA, 2014). PARs are self-starting devices, which facilitate the conversion of hydrogen and carbon monoxide into steam and carbon dioxide, respectively. Moreover, the recombiners can support the global convection and enhance the mixing in the containment atmosphere, thereby reducing local buildups of H_2/CO concentrations. Thus, recombiners are crucial elements in preventing the risk of combustion or explosion of these gases (Bachellerie et al.; Bentaib et al., 2015).

The most common PAR design consists of an array of vertical catalyst sheets located at the bottom of a rectangular housing (Fig. 1). The sheets are covered by a catalyst based on platinum or palladium, that facilitates the recombination reactions (1) and (2) that take place on the surface, by lowering the respective activation energy. Thus, reactions can occur at lower temperatures and reactant concentrations than in the non-catalysed gaseous phase.

$$H_2 + 1/2\,O_2 \rightarrow H_2O_v + 242\,kJ/mol \quad (1)$$

$$CO + 1/2\,O_2 \rightarrow CO_2 + 283\,kJ/mol \quad (2)$$

* Corresponding author.
E-mail address: araceli.dominguez@upm.es (A. Dominguez-Bugarin).

https://doi.org/10.1016/j.nucengdes.2024.113722
Received 24 July 2024; Received in revised form 16 October 2024; Accepted 15 November 2024
Available online 22 November 2024

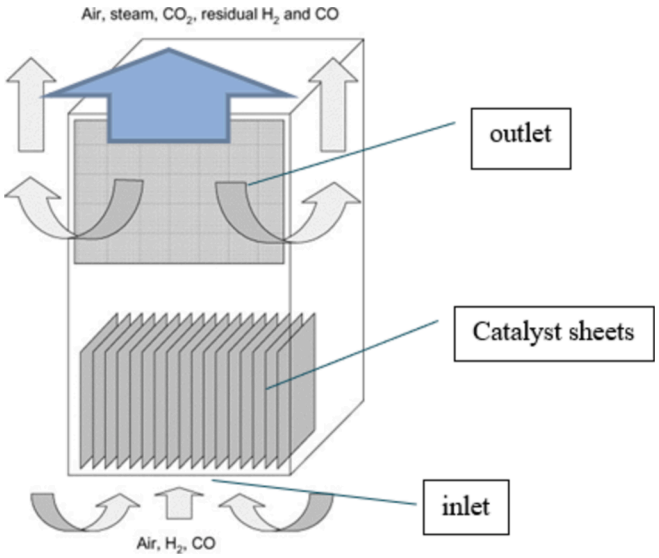

Fig. 1. Scheme of a generic PAR (Jiménez et al., 2007).

The reaction of gaseous species on the catalyst sheets is a result of different transport and reaction processes involving the gas species and the catalytic surface, which run coupled with each other: diffusion through the boundary layer of a channelled stream, adsorption/desorption on and from the active sites on the surface, and chemical reactions at the surface. The heat produced by these reactions increases the surface temperature in the heating phase, powers the reaction rates, warms the gas mixture between the catalyst sheets, and reduces the gas density through a PAR, inducing a self-sustained flow driven by natural convection. The operation of the PAR may be hindered or even prevented by the presence of poisoning species, inverse density gradients, and pressure losses through the device (Arnould, 2003).

All these phenomena must be addressed in a coupled way to accurately model the behaviour of PARs installed in nuclear reactor containment. Therefore, advanced computational codes specifically designed for PARs have been developed to simulate their performance. Comprehensive computational codes for predictive safety analyses have traditionally relied on empirical expressions that correlate the hydrogen recombination rate with environmental conditions such as temperature, pressure and reactant concentration. One example of this approach is the Framatome PAR correlation (Carcassi and Bazzicchi, 1997).

However, the applicability of these correlations is strongly dependent on the boundary conditions in the experiments from which they were derived and hence their validation is restricted to the flow conditions covered by those tests. Thus, despite the advantages of traditional empirical models in terms of low computational costs, their applicability is constrained to scenarios compatible with the range of situations from which the correlation was obtained. Hence, a need for more advanced computational tools capable of accurately predicting PAR behaviour across a broader spectrum of conditions arises (IAEA, 2011).

Mechanistic codes utilize mathematical descriptions of the physical processes occurring within the catalytic box. This approach offers a theoretical understanding of PAR behaviour and provides insights into the internal mechanisms governing recombination. The 2D mechanistic code REKO-DIREKT (Boehm, 2007), developed at FZJ, combines a numerical model of the heat and mass transfer phenomena inside the catalyst section with a generic chimney model. Thus, this model is capable of providing the local gas composition as well as the catalyst temperature profile through the PAR, although the chemical reactions on the catalyst surface are not considered in the code.

Finally, full chemistry codes solve the full set of chemical reactions in the scheme as well as describe the physical processes related to the catalytic recombiner. One example of this type of codes is SPARK (Payot et al., 2012), a 2D numerical tool developed by IRSN dedicated to catalytic reactions and recombiner modelling. The code calculates the molar concentrations in gas phase and the surface production rates with a detailed chemical mechanism that provides precise information about the conditions on the catalytic surface. Nevertheless, although this code may provide detailed information about the processes within the recombiner, the high computational cost stands as a drawback for its application to full nuclear accident transient simulations.

The European project AMHYCO (Euratom 2019-2020, GA No 945057) (Jiménez et al., 2022) aims at improving the simulation capabilities to support H_2/CO combustion risk management in severe accidents based on knowledge from experimental investigations. The project's three major goals are:

- To experimentally investigate phenomena that are difficult to predict theoretically: H_2/CO combustion and PARs behaviour under realistic accidental conditions, taking into account their interaction with safety systems.
- To improve the predictability of analysis tools –Lumped Parameter (LP), 3D and Computational Fluid Dynamics (CFD) codes– used for explosion hazard evaluation inside the reactor containment and providing support to Severe Accident Management Guidelines (SAMGs) design and development.
- To improve the Severe Accident Management Guidelines for both in-vessel and ex-vessel phases with respect to combustible gases risk management, using theoretical simulation and experimental results.

Thus, there is an interest in developing a mechanistic model that can examine in greater detail the complex processes that take place on the PAR catalytic surface and that enables dealing with evolving scenarios during a severe accident with affordable computational cost (Reinecke et al., 2010).

PARUPM is a physico-chemical code, developed at the UPM (Jiménez, 2007), that simulates the behaviour of PARs based on the surface chemistry on platinum-based catalytic surfaces as well as the heat and mass transfer processes between the catalyst and the gaseous mixtures of hydrogen, carbon monoxide, air, steam, and carbon dioxide. This code is capable of resolving the chemical reaction scheme without the high computational cost of other codes of this kind. Hence, in the context of the AMHYCO project, the PARUPM code has been proposed as a tool for simulating PARs behaviour in full containments under realistic conditions.

In this paper, a validation process of the PARUPM code as a standalone tool was performed to qualify the use of the code for severe accident scenarios. Several aspects of PARs performance (i.e., recombination rate under oxygen-rich and oxygen-lean conditions, CO poisoning in O_2-lean condition) have been evaluated in detail. This validation is performed through standalone simulations under both steady-state and transient conditions. The results obtained with the PARUPM code have been compared to experimental data obtained from both the REKO-3 facility (Reinecke et al., 2004) and the THAI containment facility (Gupta et al., 2016) program tests. Finally, a quantitative analysis between the code results and the experiments has been performed.

2. Description of the PARUPM code

PARUPM is a physico-chemical PAR code developed at the School of Industry Engineering at the Universidad Politécnica de Madrid (Jiménez, 2007). This code accounts for the various phenomena that take place in the recombiner to numerically simulate the behaviour of a PAR device. The recombiner section is conceptualized as an array of vertical flow channels separated by vertical parallel sheets with an upward vertical flow driven by natural convection passing through the channels. The code is adapted and developed for surface chemistry and heat and mass transfer between gaseous mixtures of H_2, CO, air, steam

and CO_2 and the platinum-coated parallel vertical surfaces of the recombiner section (Domínguez-Bugarín et al., 2022).

Furthermore, PARUPM is based on a simplified scheme of the surface methane combustion by (Deutschmann et al., 1996) and the Elenbaas' analysis (Elenbaas, 1942) for natural convection-induced heat transfer between parallel sheets. The analogy between mass and heat transfer is used to treat the diffusive transport to the catalyst surface.

A first validation effort was performed in (Jiménez et al., 2007) although, due to a lack of available experimental data at the time, the code was not further validated. Nowadays, and in the context of the AMHYCO project, a new modelling enhancement and validation process has been performed on the PARUPM code. This new effort may be divided in the following steps:

- The code, that was originally coupled to MELCOR 1.8.5, experienced a decoupling process. Thereby, PARUPM could be used as a stand-alone module. In this process, a new recombination rate approach based on mass diffusion was added, as well as a chimney model to get a better estimation of the PAR inlet flow velocity. This first step is described in detail in (Domínguez-Bugarín et al., 2022).
- The next step was a steady-state validation using data available from the REKO-3 test facility. In this stage, the code was further developed for simulating the behaviour of PARs under conditions typical of the late phase of a severe accident (e.g., low oxygen concentration, presence of other combustible gases such as carbon monoxide).
- Lastly, the PARUPM code was enhanced for transient conditions, i.e., the code performance was tested under evolving gas atmospheres and the associated boundary conditions. This last step was performed with data available from the THAI experiments and the capabilities of the code as a tool for simulating PARs in full containment analysis were checked.

These two last steps are explored in this work.

Surface chemistry

The code focuses on the surface reactions (heterogeneous), considering the reactions in the gas flow (homogeneous) to happen at a rate negligible in comparison. Consequently, recombination at the catalyst occurs via a reaction chain for the Pt-catalysed combustion of the species CO and H_2 adsorbed on the catalyst surface as shown in Fig. 2. These processes are described by a simplified Deutschmann model for the combustion of CH_4 on platinum catalysts through a series of 10 reactions. The reactions of the chemical model are shown on Table 1.

The table defines the values of the following parameters of the chemical reactions: the sticking factor, S_{ia}, a dimensionless parameter; the pre-exponential factor, A_i, also dimensionless; and the activation energy of the reaction, E_i^{act} in J/mol. In addition, i(s) describes the species i adsorbed on the catalyst and Pt(s) represents the presence of an active (void) site in the solid matrix where the chemical radicals are housed. The subscripts a/d indicate that the reactions are adsorption/desorption of species, respectively. Also, R is the universal gas constant.

In the PARUPM code, the desorption reactions are defined through a general Arrhenius law:

$$k_{i,d} = A_i e^{-\frac{E_{act}^i}{RT_w}} \tag{3}$$

where T_w is the surface temperature.

On the other hand, species adsorption reactions are modelled through sticking factors, $S_{i,a}$ (Table 1):

$$k_{i,a} = \frac{S_{i,a}}{\Gamma\sqrt{2\pi RTW_i}} \tag{4}$$

where W_i is the molecular weight of the specie i, and Γ is the number of sites per unit area on the catalyst surface. Meanwhile, the remaining catalytic reactions, which describe the reactions between the surface-adsorbed species, are described as general Langmuir-Hinshelwood-type mechanisms. During the whole recombination process species are being adsorbed to and desorbed from the active sites (Fig. 2). The availability of hydrogen, oxygen and carbon monoxide on the catalyst surface and their proportions determine the recombination rate of the process. The adsorption and desorption of species depend highly on the surface temperature T_w. The full description of the modelling implemented in the PARUPM code can be found in (Domínguez-Bugarín et al., 2022).

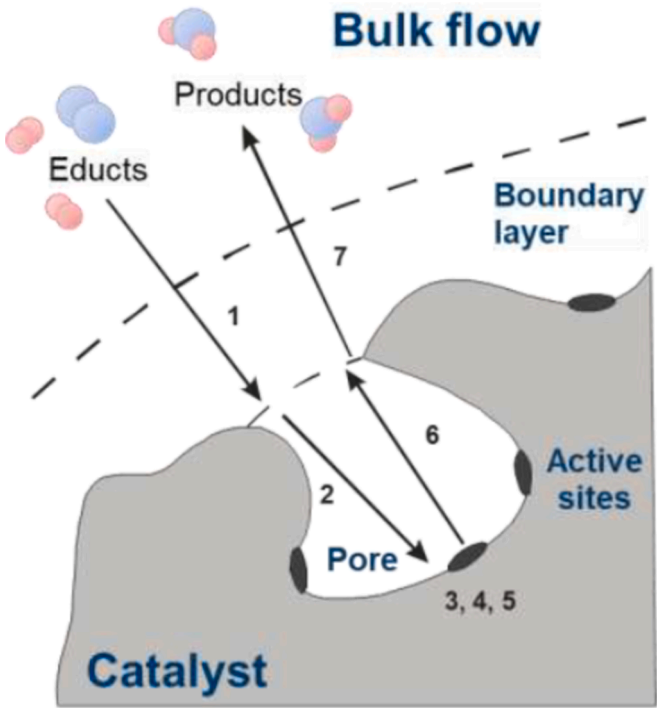

Fig. 2. Simplified scheme of active sites occupancy on a catalyst material (Reinecke, 2023). Reactants (H_2 and CO) are (1) diffused through the boundary layer, (2) absorbed on the active site, (3,4,5) chemical reactions take place on the site, (6) products are desorbed, and (7) products are diffused through the boundary layer.

Table 1
Reactions scheme based on a simplified Deutschmann combustion model for methane catalysed with Pt (Deutschmann, 1996).

Elemental Reaction	S_{ia}	A_i	E_i^{act} (J/mol)
1a) $H_2 + 2Pt(s) \rightarrow 2H(s)$	0.046	–	–
1d) $2H(s) \rightarrow H_2 + 2Pt(s)$	–	3.7×10^{17}	$R(8110\text{-}722\theta_H)$
2a) $O_2 + 2Pt(s) \rightarrow 2O(s)$	$0.07\times (300/T)$	–	–
2d) $2O(s) \rightarrow O_2 + 2Pt(s)$	–	3.7×10^{17}	$R(25631\text{-}7220\theta_O)$
3a) $H_2O + Pt(s) \rightarrow H_2O(s)$	0.75	–	–
3d) $H_2O(s) \rightarrow H_2O + Pt(s)$	–	10^{13}	40,300
4) $H(s) + O(s) \rightarrow OH(s) + Pt(s)$	–	3.7×10^{17}	11,500
5) $H(s) + OH(s) \rightarrow H_2O + Pt(s)$	–	3.7×10^{17}	17,400
6) $OH(s) + OH(s) \rightarrow H_2O + O(s)$	–	3.7×10^{17}	48,200
7a) $CO + Pt(s) \rightarrow CO(s)$	0.84	–	–
7d) $CO(s) \rightarrow CO + Pt(s)$	–	10^{13}	125,500
8d) $CO_2(s) \rightarrow CO_2 + Pt(s)$	–	10^{13}	20,500
9) $CO(s) + O(s) \rightarrow CO_2(s) + Pt(s)$	–	3.7×10^{17}	105,000
10+) $C(s) + O(s) \rightarrow CO(s) + Pt(s)$	–	3.7×10^{17}	62,800
10-) $CO(s) + Pt(s) \rightarrow C(s) + O(s)$	–	10^{14}	184,000

3. Description of experimental facilities

To help in the development and validation of safety codes, as well as in the general design and enhancement of passive mitigation systems, international projects have focused on accident-typical conditions in the containment of a water-cooled reactor. These experiments have been envisaged and performed to establish a database that allows producing better models that simulate the behaviour of a recombiner. In this work, the analysis was focused on the databases provided by the REKO-3 facility (Reinecke et al., 2004) at Forschungszentrum Jülich GmbH (FZJ) and the THAI (Gupta et al., 2016) program tests performed by Becker Technologies GmbH.

3.1. REKO-3

The compact-scale test facility REKO-3 (Reinecke et al., 2010), developed FZJ and shown in Fig. 3, serves as a dedicated platform for the detailed examination of catalyst samples within a vertical flow channel. The experimental setup provides well defined conditions for the gas mixture composition, flow rate, and inlet temperature.

The key element of this set-up is a vertical rectangular flow channel equipped with 4 catalytic sheets. These sheets are composed of stainless steel with a ceramic wash coat containing platinum. The flow channel outlet section leads into an exhaust-air stack. This configuration mimics a box-type recombiner section, based on the Framatome design principles. A well-defined gas mixture, which is composed of air, hydrogen, nitrogen (to obtain oxygen-lean conditions), carbon monoxide, and steam is supplied at the channel inlet and monitored by means of mass flow controllers. This gas mixture flows at a pre-defined velocity through the catalyst section (Reinecke et al., 2022).

The primary objective of the REKO-3 experiments is to study the relevant processes occurring on plate-type catalysts (Reinecke et al., 2004). For this purpose, the natural convection effect occurring in a real PAR is intentionally removed by imposing predefined forced flow conditions. As a result, the experimental data obtained from this facility authentically represent the performance of a recombiner under steady-state conditions. It is worth noting that the pressure in REKO-3 experiments is always the ambient pressure, i.e., there is not a force pressure added to the experiment since it is an open channel, and the temperature will depend on the inlet conditions for each individual test.

The plate temperature is measured with thermocouples located at different vertical positions inside the catalyst plate while the outlet concentrations are measured with a gas analyser.

3.2. THAI facility

The test facility THAI (thermal-hydraulics, hydrogen, aerosol, and iodine) (NEA, 2010), operated by Becker Technologies GmbH, addresses open questions concerning gas distribution, behaviour of hydrogen, iodine and aerosols in the containment of light water reactors during severe accidents. Since 2000, several series of experimental campaigns, funded by national and international projects (Gupta et al., 2021), have been performed. Their main objective is to provide containment-specific experimental databases for the development and validation of LP and CFD codes in the context of reactor safety analyses. This facilitates the investigation of specific issues for light water reactors (LWR) under severe accident conditions, i.e. thermal hydraulics, hydrogen distribution, combustion, and mitigation, as well as fission product behaviour.

In the context of the international project OECD/NEA THAI (Gupta et al., 2016) and THAI National project (Freitag et al., 2020), a series of experiments involving hydrogen recombination (HR) tests were conducted over the past decade. These tests systematically varied factors such as initial thermal–hydraulic conditions (i.e. pressure, temperatures, steam concentrations, etc.) to investigate the onset of recombination, recombination rate and ignition potential under ambient/saturated/superheated steam atmospheres and elevated initial pressure and temperature conditions. The effect of O_2 starvation, a phenomenon expectable during the late phase of severe accidents, was also studied (Bentaib et al., 2015), as well as the influence of thermal–hydraulic conditions on the oxidation of carbon monoxide on the catalyst sheets and the effect of CO on the H_2 recombination rate under normal operating and oxygen starvation conditions (Freitag et al., 2020). Several of the recombiner experiments performed in the aforesaid experimental programs were used for the validation exercise in this work.

The main component of the THAI facility is a 60 m^3 stainless steel vessel, 9.2 m high and 3.2 m in diameter, with removable internals for multi-compartment investigations (Fig. 4 left). In the case of the HR tests, an inner cylinder is located in the centre of the main vessel and the recombiner is placed at the outer wall of this cylinder (Fig. 4 right).

Tests considered for the PARUPM code validation were performed with a Framatome FR90/1-380 T (Framatome, 2024) recombiner with a 50 % reduction of both the inlet cross-section and the number of catalyst sheets. All tests were run with a first injection phase of combustible gases, a subsequent depletion phase, a second gas injection phase, and a second and last depletion phase. The tests selected for the transient PARUPM validation were the HR-2 and HR-12 from the OECD/NEA-THAI project, as well as the tests HR-51 and HR-53 from the THAI National project.

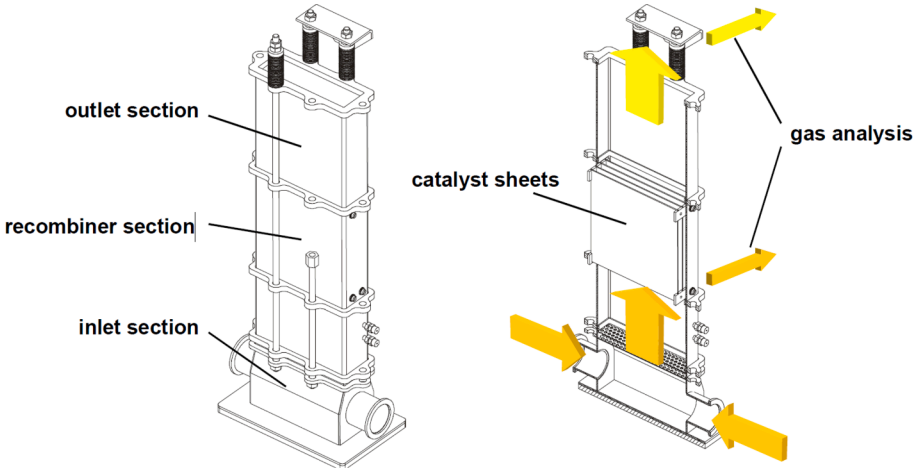

Fig. 3. Scheme of the modular setup of the REKO-3 flow channel (left) and the internal flow paths (right). (Bachellerie et al.).

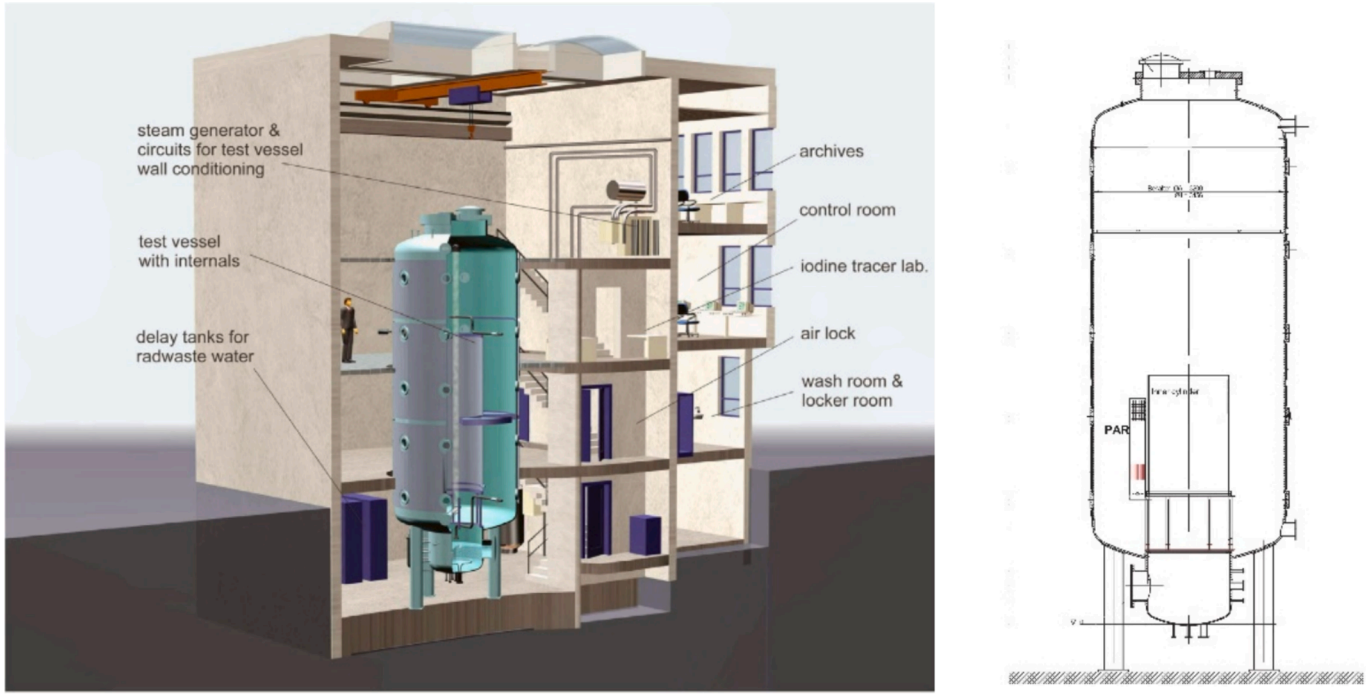

Fig. 4. THAI test facility (Gupta et al., 2016) and scheme of the vessel for the HR tests.

4. Standalone code validation

The validation of the PARUPM code as a standalone module has been performed in two stages: the first one is a validation under steady-state conditions and the second one a validation under transient conditions.

4.1. Steady-state validation

The first step in the validation process consisted of analysing the code capabilities for phenomena expected during the ex-vessel phase of severe accidents, i.e., O_2 starvation and CO recombination. Using the data from REKO-3 experiments, the code was adapted to better suit the behaviour of a recombiner under conditions of lean oxygen availability with the presence of carbon monoxide.

4.1.1. Recombination rate

First, an enhancement process on the PARUPM code was performed. Originally, the recombination rate calculated by PARUPM was based on the surface reaction. Studies have shown that under stable catalyst temperature conditions the recombination process is primarily driven by the diffusion of species through the boundary layer (Reinecke et al., 2010). Thus, although the code calculates the recombination rate by both diffusion and chemical reaction processes, the final value chosen for the recombination rates is the one obtained with the diffusion model, since it is the most restrictive one. This decision is supported by the results shown in (Domínguez-Bugarín et al., 2022) where more accurate results are obtained once the diffusion model is considered for calculating the recombination rate instead of the chemical reaction rate.

4.1.2. O_2 starvation

To study the effect of oxygen starvation on PAR performance (i.e., low oxygen concentrations are available in the surrounding area reducing the overall recombination rate and impacting the efficiency of the device), experiments where the oxygen molar fraction was progressively reduced have been analysed. In these experiments (Reinecke et al., 2007), the H_2 molar fraction in the gas mixture was kept constant at 3 % while the O_2 molar fraction was reduced from a 20 % gradually to a 2 % of the total volumetric flow rate. The flow speed was kept constant at 1.15 m/s and the H_2 recombination rates were obtained for gas temperatures at the inlet of 20.5 °C and 80.1 °C. The tests analysed in this study are shown on Table 2.

To study this effect with PARUPM, a critical oxygen concentration threshold value $X_{O_2,crit}$ may be determined (Equation 5). If $X_{O_2} > X_{O_2,crit}$ the recombiner will not operate in oxygen starvation conditions. Nevertheless, if $X_{O_2} < X_{O_2,crit}$, O_2 will be treated as the limiting parameter for the recombination which could lead to a reduction of the recombination rate. As defined in (Klauck et al., 2021), the critical oxygen concentration value can be calculated as:

$$X_{O_2,crit} = \frac{1}{2}\left[\left(\frac{D_{H_2}}{D_{O_2}}\right)^{2/3} X_{H_2} + \left(\frac{D_{CO}}{D_{O_2}}\right)^{2/3} X_{CO}\right] \quad (5)$$

where D_i is the molecular diffusive coefficient of the specie i, and X_i is the molar fraction of the gas.

Fig. 5 left shows the recombination rate obtained for the inlet temperature of 20.5 °C with both PARUPM and REKO-3, and Fig. 5 right the recombination rates for the inlet temperature of 80.1 °C. In both cases, the code reproduces well the behaviour when the recombiner experiences O_2 starvation). In both sets of tests, this phenomenon occurs for test 5, i.e., the case when the oxygen concentration goes below the H_2 concentration.

Table 3 shows the relative differences, ΔHrate, between the recombination rates obtained with PARUPM and the experimental results. In general, these differences go below 15 % independently of the inlet O_2 concentration and temperature. Furthermore, PARUPM can correctly predict when the PAR is operating under oxygen starvation conditions using the expression given in equation 5.

For each case, $X_{O_2,crit}$ was calculated by PARUPM using inlet conditions. The code was capable of determining that, for both tests oxygen

Table 2
Tests analysed classified by O_2 concentrations.

	Test 1	Test 2	Test 3	Test 4	Test 5
T = 20.5 °C	20 % XO_2	5 % XO_2	4 % XO_2	3 % XO_2	2 % XO_2
T = 80.1 °C	20 % XO_2	5 % XO_2	4 % XO_2	3 % XO_2	2 % XO_2

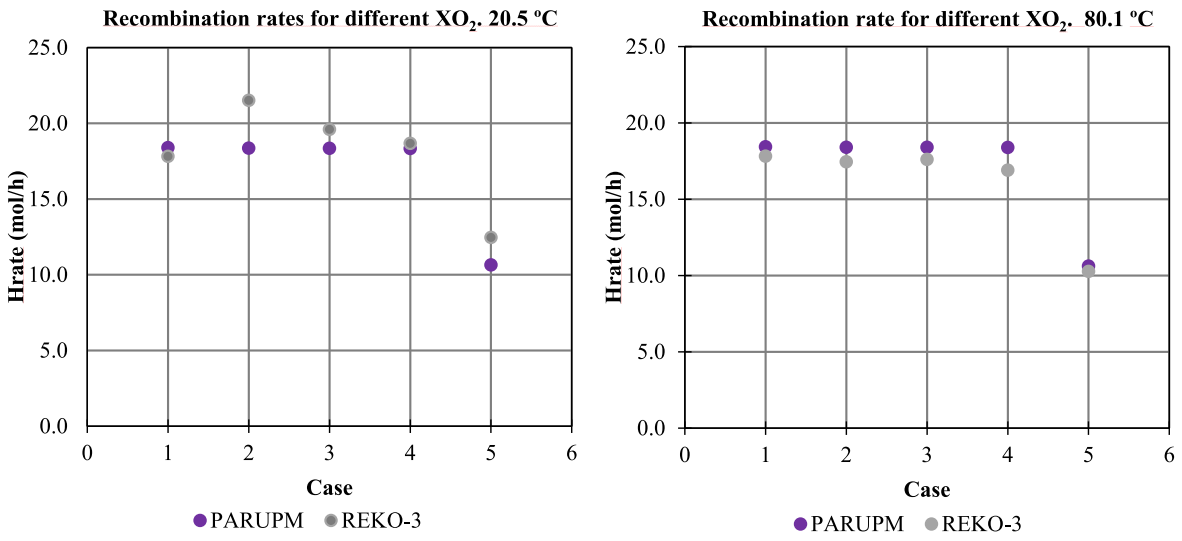

Fig. 5. Recombination rates obtained with PARUPM and from REKO-3 for different O_2 concentrations and inlet temperatures.

Table 3
Recombination rates obtained with PARUPM and from REKO-3 for 5 different O_2 concentrations and 2 inlet temperatures.

X_{O2}	T(°C)	H_{rate} PARUPM (mol/h)	H_{rate} REKO-3 (mol/h)	ΔH_{rate}
0.20	20.50	18.40	17.82	0.03
0.05	20.50	18.36	21.52	0.15
0.04	20.50	18.35	19.60	0.06
0.03	20.50	18.34	18.68	0.02
0.02	20.50	10.65	12.46	0.15
0.20	80.10	18.43	17.82	0.03
0.05	80.10	18.41	17.45	0.06
0.04	80.10	18.40	17.61	0.04
0.03	80.10	18.40	16.91	0.09
0.02	80.10	10.62	10.27	0.03

starvation is experienced by the PAR in case 5, since the recombination rate is drastically reduced. Recombination rates were then calculated taking into account this phenomenon. Hence, the code is capable of predicting with fair accuracy when the PAR is operating under oxygen starvation conditions and the recombination rates once this stage is reached.

4.1.3. *Effect of carbon monoxide*

To study the effect of CO on the H_2 recombination rate and the catalyst temperature, and to analyse the CO recombination capability of the code, several REKO-3 experiments were analysed from the series R3-A-03_CO, R3-A-04_CO, and R3-A-06_CO (Klauck et al., 2014). In these tests, three different H_2 concentrations, and other three different CO concentrations where studied. In these tests, the inlet flow temperature was kept at 21°C for all the experiments and the flow velocity was 1.15 m/s for every run. The O_2 concentration for each run is $X_{O_2} = (100 - X_{H_2} - X_{CO}) \bullet 0.21$ and the mixture is dry, i.e., there is no steam in the injected gas mixture.

- Series 1: 2 % H_2 for 0 %, 0.5 %, 1 %, and 2 % CO.
- Series 2: 4 % H_2 for 1 %, 2 %, and 4 % CO.
- Series 3: 5 % H_2 for 1 %, 2 %, 3 %, 3.5 %, and 4 % CO.

Based on H_2 and CO flammability limits (4 % and 12.5 % respectively), and using the LeChatelier rule to calculate the flammability limit of the H_2/CO mixture, the atmospheres of tests performed in series 2 and 3 could be flammable (Coward and Jones, 1952). Since PARUPM does not possess a module for simulating ignition nor there was an ignition during the performance of these experiments, this phenomenon was not considered for this analysis.

As shown in Fig. 6, the average relative code-test deviation for the H_2 recombination rates is ~ 5.4 % while the average deviation for the CO recombination rates is ~ 15.4 %. It is worth noting that both recombination rates are calculated simultaneously and that the code is addressing the competing effects of both H_2 and CO reacting with O_2. Thus, larger deviations between experimental and simulated recombination rates are expected. Nevertheless, within these limits, the model is considered capable of calculating the recombination rates of both species in the presence of CO.

For the catalyst temperature, shown in Fig. 7, we compared the average experimental plate temperature with the calculated plate temperature given by PARUPM. The relative code-test deviation is ~ 3.0 % with a homogeneous distribution on this deviation. Thus, the code predicts well the catalyst temperature in a wide range of concentrations. Within these limits, the code is considered capable of calculating the catalyst temperature in the presence of CO.

4.2. *Transient mode*

Once the code was optimized for steady-state conditions, the next step in the validation program was to analyse the behaviour of the code under transient conditions. The information available from experiments of the series HR performed in the THAI facility has been used for this purpose (NEA, 2010; Gupta et al., 2019). The data obtained with the code has been compared with the experimental results for several relevant parameters, i.e., outlet gas concentrations, catalyst temperatures, and flow velocity, since these parameters are directly extracted from the experiment. The boundary conditions for the simulations (i.e., pressure, inlet gas temperature and inlet gas concentrations) are given directly to the code. These values have been peaked from sensors located in the experiment in the region close to the PAR inlet and given to the PARUPM code at each time step of the simulation. The velocity is calculated by PARUPM through a chimney model using these boundary conditions at the inlet of the PAR and the geometric information of the simulated PAR.

4.2.1. *Recombination rates: HR-2*

Test HR-2 starts with a vessel atmosphere of dry air at an ambient temperature of 25 °C at 1 bar. During the first phase of the test, H_2 is injected in the vessel and the recombination begins once the H_2 concentration reaches 1.15 % at the PAR. After 25 min, the injection stops and a first depletion phase starts, which is let to evolve for 60 min. Then, the second hydrogen injection phase takes place with a duration of 20 min followed by the second depletion phase which runs until the

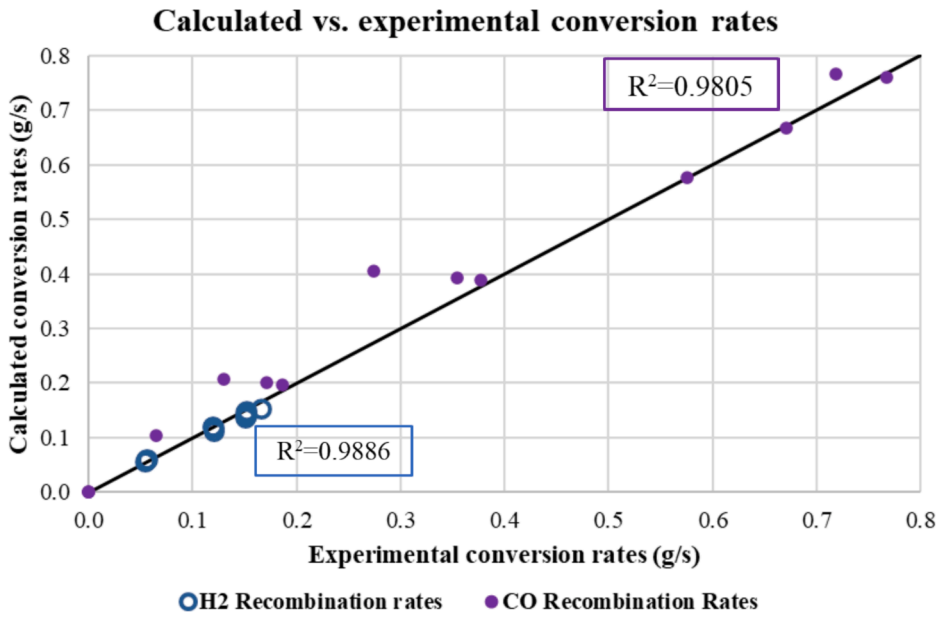

Fig. 6. PARUPM H_2 and CO recombination rates against experimental recombination rates in g/s for the REKO-3 tests with carbon monoxide.

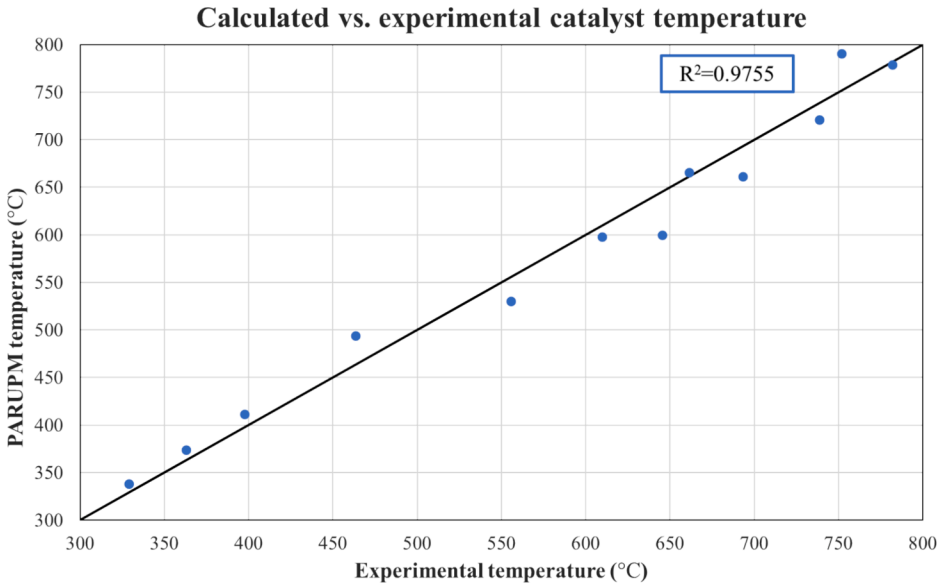

Fig. 7. PARUPM catalyst temperature against experimental in °C for the REKO-3 tests with carbon monoxide.

recombination ends when H_2 concentration reaches a 0.3 % (Kanzleiter, 2009a).

Fig. 8 shows the experimental results for the H_2 concentration at the outlet section of the device, the catalyst temperature, and the flow velocity for the experiment HR-2 compared to the values obtained with PARUPM. The most significant discrepancy between the code and the experiment regards the outlet H_2 concentration at the end of the second injection phase (at around 90 min), which is due to a PAR-induced ignition in the PAR causing lower outlet H_2 concentrations in the experiment. PARUPM does not contain an ignition module, therefore, this behaviour cannot be captured by the code.

The predicted average catalyst temperatures are higher than the experimental ones during both depletion phases. One possible explanation could be that the PARUPM code does not consider heat transfer phenomena, such as the effect of radiative heat exchange between the catalyst sheets and the metallic structure of the recombiner, as well as between the PAR housing and the vessel walls.

The flow velocity is well captured during the first depletion phase. However, the effect of the ignition during the second depletion phase is not well captured by the flow velocity module, thus the velocity during the second depletion follows a pattern similar to the first depletion in the simulation.

4.2.2. O_2 starvation: HR-12

The initial conditions of test HR-12 include a mixture of air with 60 vol% steam at a temperature of 86 °C and a higher pressure of 3 bar. The test follows the same pattern of injection and depletion as HR-2. However, during the second injection and depletion phases, the recombination runs under oxygen starvation conditions starting at 125 min, when $X_{O_2}/X_{O_2,crit} < 1$. H_2 injection does not stop until 170 min after the beginning of the transient (hence the observed plateau between 125 and 170 min in Fig. 9 left). After 170 min the second depletion starts. A third

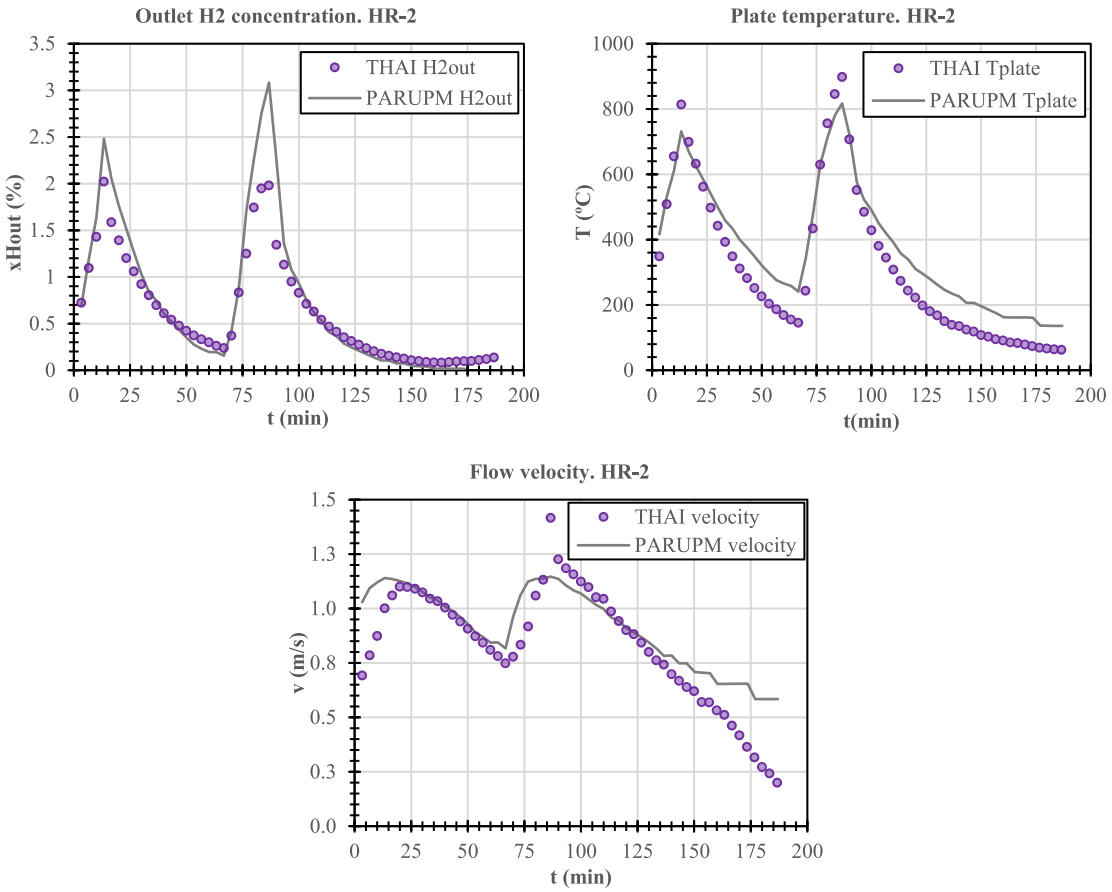

Fig. 8. H_2 outlet concentrations, catalyst temperature, and flow velocity with PARUPM and the corresponding experimental values during the HR-2 transient in the THAI facility.

shorter injection of H_2 at around 252 min is also performed to further confirm the oxygen starvation effect observed. These conditions are more similar to what is expected to reach during the late phase of a severe accident transient (Kanzleiter, 2009b).

Fig. 9 also shows the outlet H_2 concentration, the catalyst temperature, and the flow velocity obtained from the experiment HR-12 and the corresponding values calculated with PARUPM using the boundary conditions from the experiment. The figure shows that the code reproduces fairly well the behaviour of a realistic PAR inside a containment during the second injection and depletion phases (as well as the rest of the transient), when the recombiner is experiencing oxygen starvation.

The same issue appears with the heat transfer in this experiment, although the effect is less pronounced when the recombiner reaches O_2 starvation conditions, i.e., during the second depletion phase. Therefore, the code is able to predict the average catalyst temperature in conditions similar to a late phase severe accident.

Finally, the flow velocity calculated with PARUPM for this experiment shows the expected behaviour compared to the experimental values. Both depletion phases as well as the second injection are accurately reproduced with the model. The only significant discrepancy found is during the first injection phase where the calculated velocity is higher than the experimental one.

Nevertheless, once the recombiner reaches quasi steady-state conditions (second depletion) the code is capable of simulating the behaviour of a real recombiner in conditions similar to the late phase of a severe accident.

4.2.3. CO impact: HR-51, HR-53

The next step in the validation effort was to study the behaviour of the PARUPM code during transients with the presence of CO. Experiments HR-51 and HR-53 have been selected for this purpose. Both experiments follow the same pattern of injection and depletion phases and can be compared to HR-2 and HR-12 respectively due to their equal initial conditions (Freitag et al., 2020). Table 4 shows the concentrations at the PAR inlet of H_2, O_2, H_2O, CO, and CO_2 for HR-2, HR-12, HR-51, HR-53 after the second injection to emphasize the similarities among these experiments. The presence of CO affects the recombination, thereby the study is focused on the capabilities of the code for simulating transients where the presence of CO is relevant. Preliminary works with HR-51 showed that the code was not capable of solving the numerical scheme once the conditions at the catalyst were close to CO poisoning. Under these conditions, the presence of CO disables the recombination process by occupying all the available sites at the surface, and this effect is more pronounced at low catalyst temperature (very low CO desorption rate, Fig. 11 right). Consequently, a criterion has been established to allow the code to resolve the model once this condition is reached.

4.3. CO poisoning criterion

Since experiment HR-51 reached a state of CO poisoning, a switch for this phenomenon was implemented in the code to let its advance for a time step. As PARUPM uses a physico-chemical approach (Jiménez et al., 2007), the surface concentrations of the different species present are calculated for every time step.

Fig. 10 shows a histogram of the percentage of occupancy of hydrogen (z_H), oxygen (z_O), hydroxyl radicals (z_{OH}), carbon monoxide (z_{CO}), and free sites (z_ν) for the HR-51 transient. Once the catalyst sheet is heated by the initial H_2 and CO recombination, the active sites of the catalyst are nearly completely occupied by oxygen (z_O close to 1), with a

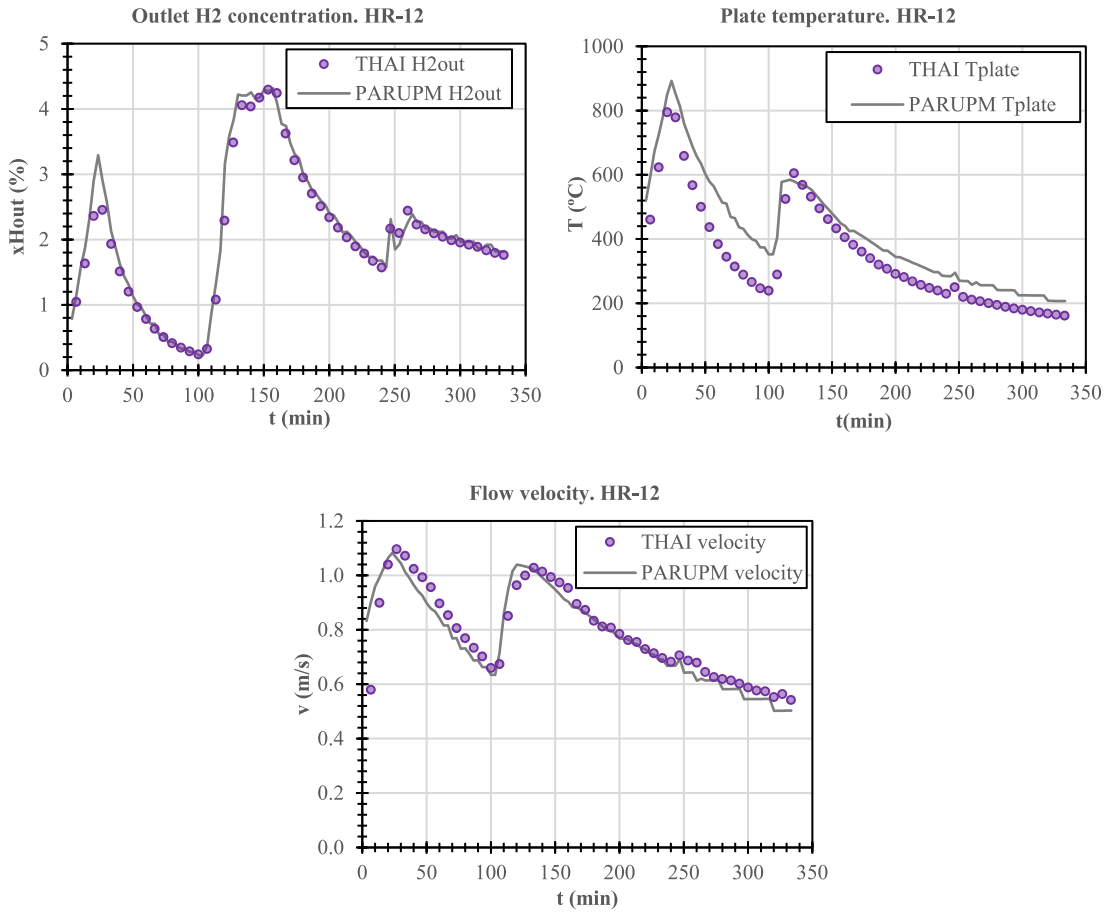

Fig. 9. H_2 outlet concentrations, catalyst temperature, and flow velocity with PARUPM and the corresponding experimental values during the HR-12 transient in the THAI facility.

Table 4
H_2, O_2, H_2O, CO, and CO_2 concentrations at the PAR inlet for tests HR-2, HR-12, HR-51, HR-53 after the second injection ends.

	XH_2 (%)	XO_2 (%)	XH_2O (%)	XCO (%)	XCO_2 (%)
HR-2	6.8	17.2	0.0	0.0	0.0
HR-12	5.2	2.4	61.8	0.0	0.0
HR-51	5.9	15.7	1.8	1.3	1.0
HR-53	4.2	2.8	62.2	0.7	1.0

small percentage of sites occupied by CO and H_2. This very low fraction cannot be seen on the histogram, namely all the CO and H_2 are absorbed and instantly recombined since the limiting factor for the recombination rate is not the rate of the CO/O_2 and H_2/O_2 reactions but the supply of these species to the surface governed by diffusion from the bulk through the boundary layer (Reinecke et al., 2010).

The injection of CO and H_2 stops 16 min after the beginning of the recombination. At that point, the oxygen covers the majority of the available sites in the surface. Recombination is happening at a faster rate than the diffusion of the species because of the still high catalyst temperature, thus new vacant sites are made available. Once this injection phase stops, the recombination gets slower since the H_2 and CO available in the atmosphere get leaner. Once the catalyst temperature falls below a threshold value of around 180 °C, the fraction of site occupancy by oxygen is gradually substituted by the CO molecules, thereby putting the recombination rate down.

Once the oxygen occupation decreases below 60 % of the total available sites, the recombiner is considered poisoned and the recombination stops. In HR-51, this phenomenon happened 100 min after the transient started. This is shown in Fig. 11, where the catalyst temperature drops down to ambient temperature around that time on the lower part of the sheet. Hence, the bottom part of the catalyst is experiencing poisoning. The middle part gets poisoned at around 115 min, and the upper part at around 125 min.

The second injection starts at around 120 min after the beginning of the recombination. At this point, the recombiner shows the same behaviour as in the first injection, i.e., the recombiner is capable of recovering performance after experiencing CO poisoning. The active sites are rapidly occupied by oxygen once the recombination is restarted and stabilised. Again, all the CO and H_2 that are reaching the catalyst surface are recombined and the available sites are either occupied by O (the majority) or vacant. During the second injection an ignition is produced in the recombiner, but this effect is not captured on the surface chemistry model as explained above.

Again, the recombination process starts to decelerate once the H_2 and CO concentrations in the mixture get leaner. As in the first depletion, once the surface coverage reaches an O occupation below 60 % of the available sites, the catalyst is poisoned by CO, which occupies all the available sites and displaces the oxygen.

As a consequence, a CO poisoning criterion may be established in the PARUPM code. This criterion will limit the recombination rate once the surface coverage reaches a certain threshold value of critically low O concentration in the catalyst surface, which has been set to a fraction of 0.60. To account for the fact that not all the catalyst gets poisoned simultaneously, a delay on the poisoning has been added as well. This value has been tested with experiments HR-51 and HR-53. Now, validations of transients with CO, e.g. HR-51 and HR-53, can be performed with the model to further validate PARUPM.

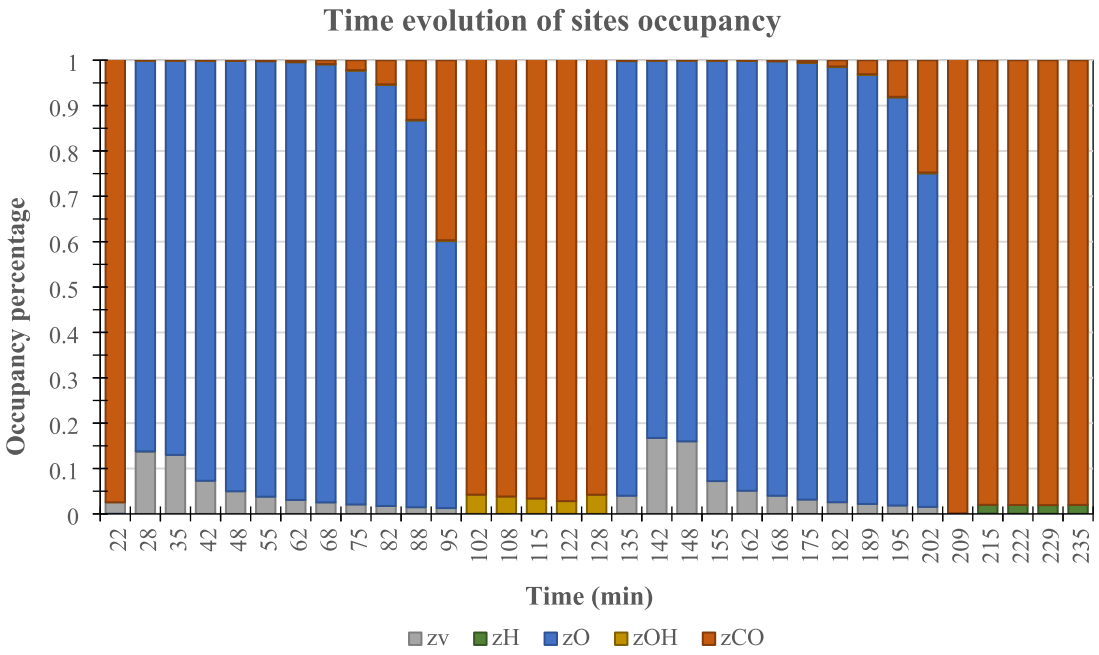

Fig. 10. Site occupancy of different species on the active surface against time for HR-51.

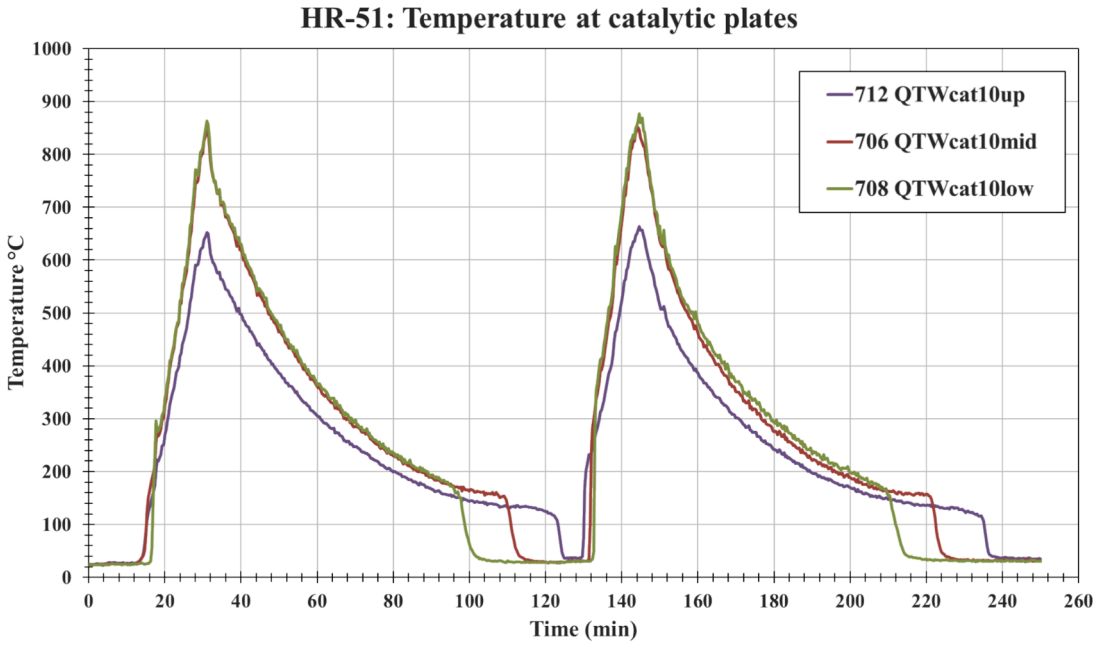

Fig. 11. Surface temperatures for HR-51 for the middle sheet at 3 locations: the bottom of the sheet (green line), the middle of the sheet (red line), and the top (purple line) (Gupta et al., 2019).

Substituting the values from Table 1 into equations (3) and (4), the adsorption and desorption coefficients for both CO and O_2 over the catalyst surface can be calculated as a function of the catalyst temperature T_w. Fig. 12 (left) and 12 (right) show the adsorption and the desorption coefficients for these species vs the catalyst temperature. The adsorption coefficients for both species depend on the catalyst temperature, although this dependency is more pronounced for O_2. In Fig. 12 (left) we can see that while the slope is more pronounced for the adsorption of O_2 than for the CO.

The desorption coefficients are more dependent on temperature since they follow an Arrhenius law, with CO desorption being the most sensitive to temperatures, especially in the lower range. In Fig. 12 (right), we can see that the desorption coefficient decreases eight orders of magnitude between 400°C and 100°C, whereas for oxygen only drops four. Hence, CO tends to desorb slower from the catalyst at lower temperatures than O_2. Lower desorption coefficients mean that the CO is not being desorbed from the surface, thereby the available sites of the catalyst are occupied by CO for a longer time. If the catalyst temperature gets even lower with time, the desorption coefficient for CO is so low that CO is covering all the active sites available, causing the poisoning of the catalyst.

Nevertheless, if the catalyst temperature increases, CO will desorb faster. This will lead to more sites being available for the catalytic reactions. These reactions will increase the catalyst temperature,

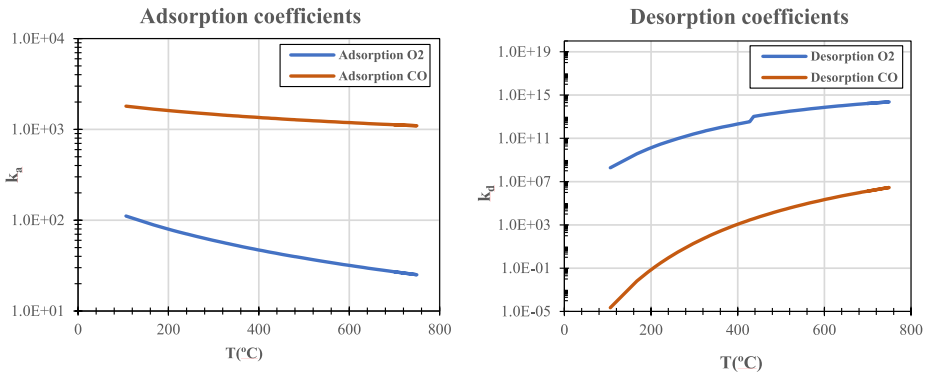

Fig. 12. Adsorption and desorption coefficients for CO and O_2 vs surface temperature.

accelerating CO desorption which leads to more O and H radicals being absorbed into the catalyst. If this tendency is kept, CO will quickly desorb, effectively depoisoning the catalyst. Thus, CO does not have a permanent effect on the catalyst. Once the O concentration is higher than 0.60, PARUPM will assume that the catalyst is no longer poisoned, and the recombination will be calculated again.

4.4. Simulation of HR-51 and HR-53

The initial conditions of test HR-51 include a mixture of H_2 and CO, with a ratio 4 to 1, at a temperature of 25 °C and a pressure of 1.5 bar and dry air, hence similar conditions to HR-2. In this test, conditions of O_2 starvation were not reached, however the catalyst experiences CO poisoning during the late phase of both depletion phases when the catalyst temperature decreases below a threshold temperature (Gupta et al., 2019).

Fig. 13 shows the outlet concentrations of both CO and H_2 for test HR-51, as well as the catalyst temperature and the flow velocity. The outlet concentrations of both H_2 and CO have been calculated with PARUPM and compared with the experimental results. From this comparison PARUPM shows its capability for calculating the recombination rate of both gases simultaneously. The CO concentration is particularly well determined by the code. The H_2 recombination is slightly overestimated in both depletion phases (the H_2 concentrations at the outlet of the recombiner are lower than measured in the test). Furthermore, during the second injection (at around 140 min), an ignition occurred,

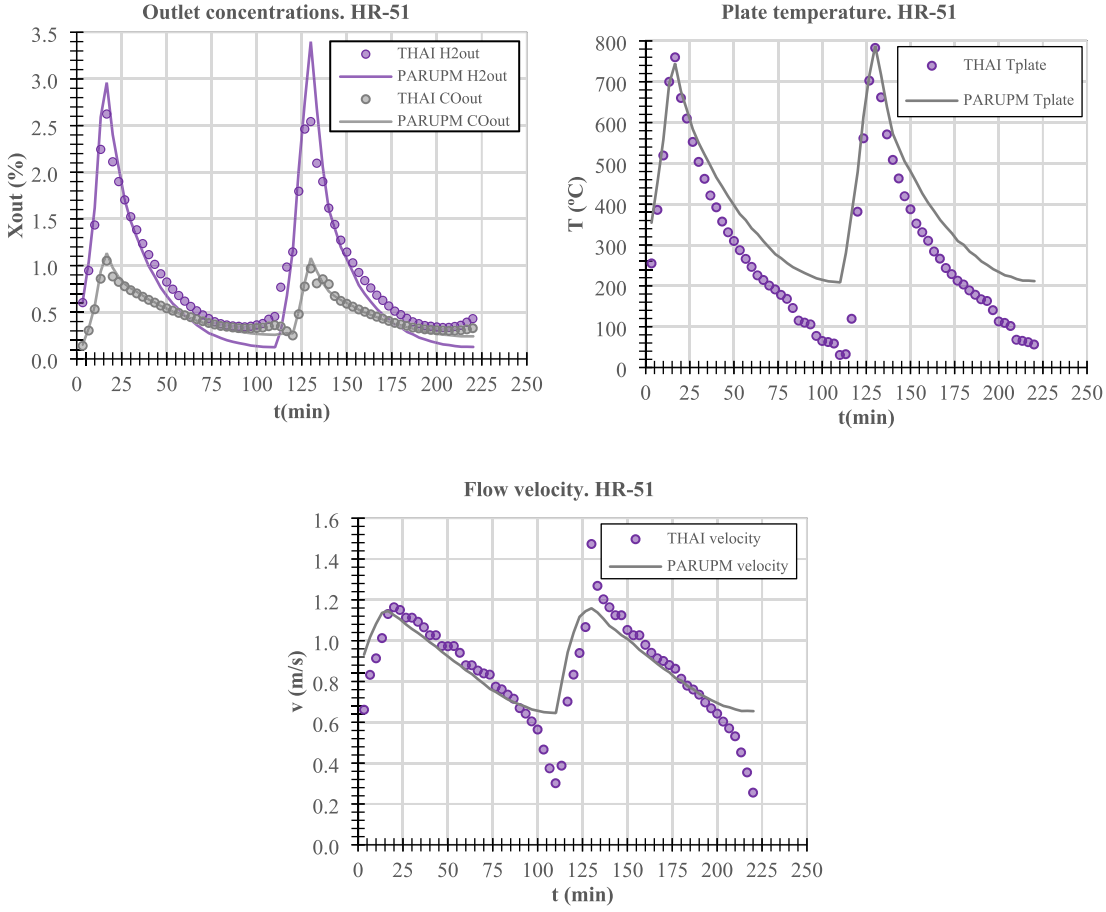

Fig. 13. H_2 and CO concentrations at the outlet of the PAR, catalyst temperature, and flow velocity with PARUPM and the corresponding experimental values during the HR-51 transient in the THAI facility.

thus the outlet H_2 concentration at the end of the second injection phase is higher than the test one since the code is not simulating the combustion of the excess H_2. Either way, the total recombined H_2 mass from this test has a standard deviation of less than 4.7 %.

The catalyst temperature faces the same issues as in HR-2. Both depletion phases show slightly overpredicted catalyst temperatures, which may also explain the overestimation of the H_2 recombination rates during these phases. This could be caused by the fact that the code does not consider some phenomena related to the heat transfer from the sheets to external structures, such as the casing or the vessel. Namely, the effect of radiative heat loss to the other sheets and the metallic structure of the recombiner or the conductive heat loss through the casing are neglected. The CO poisoning that starts at 115 min on the middle part of the catalyst (Fig. 11) is captured by the code. Finally, regarding the flow velocity through the PAR, there is a slight overestimation during the injection phases but overall, flow velocities are well estimated during the depletion phases. During the poisoning periods a threshold flow velocity is stablished to avoid convergence errors.

The initial conditions of test HR-53 include a mixture of air with 60 vol% steam, and H_2 and CO at a 7/1 ratio, a temperature of 86 °C and a higher pressure of 3 bar. The test follows the same pattern of injection and depletion phases as HR-12. Accordingly, during the second injection and depletion, the recombination runs under oxygen starvation conditions, as well as the effect of the presence of CO on the mixture. The second injection does not stop until 280 min after the beginning of the transient (hence the observed plateau between 250 and 280 min in Fig. 14 left). After 280 min the second depletion starts. A third shorter injection of H_2 at around 330 min is also performed to further confirm the oxygen starvation effect observed and to avoid CO poisoning. These conditions are similar to those expected during the late phase of a severe accident, although the CO concentration in vol.% is 7 times smaller than the H_2 concentration (Gupta et al., 2019).

Fig. 14 shows the outlet concentrations of both CO and H_2 for test HR-53, as well as the catalyst temperature and the flow velocity. Both outlet concentrations are well captured by the model. During the late phase of the second depletion phase the H_2 outlet concentration is lower than the experimental one, i.e., the calculated recombination rate is higher than the real one. In this part of the transient, the recombiner is experiencing severe O_2 starvation, as well as lean conditions of both H_2 and CO. Thus, the code captures well the outlet concentrations (recombination rates) of both gases even with O_2 starvation. Furthermore, the total recombined H_2 mass deviation is of less than 4.2 %.

As in the previous cases, the catalyst temperature is overestimated during the depletion phases, mostly during the first one. As in HR-12 (Fig. 9), once the recombiner reaches O_2 starvation conditions (i.e., during the second depletion phase) the catalyst temperature is not overpredicted. Thus, the code is capable of predicting the catalyst temperature even when the recombiner under the effects of both O_2 starvation and CO.

Finally, the flow velocity calculated with PARUPM for this experiment shows the expected behaviour compared to the experimental values. Both injection phases as well as the first depletion are accurately reproduced with the model. The only significant discrepancy found is during the second depletion phase where the calculated velocity is slightly lower than the experimental one during the transient.

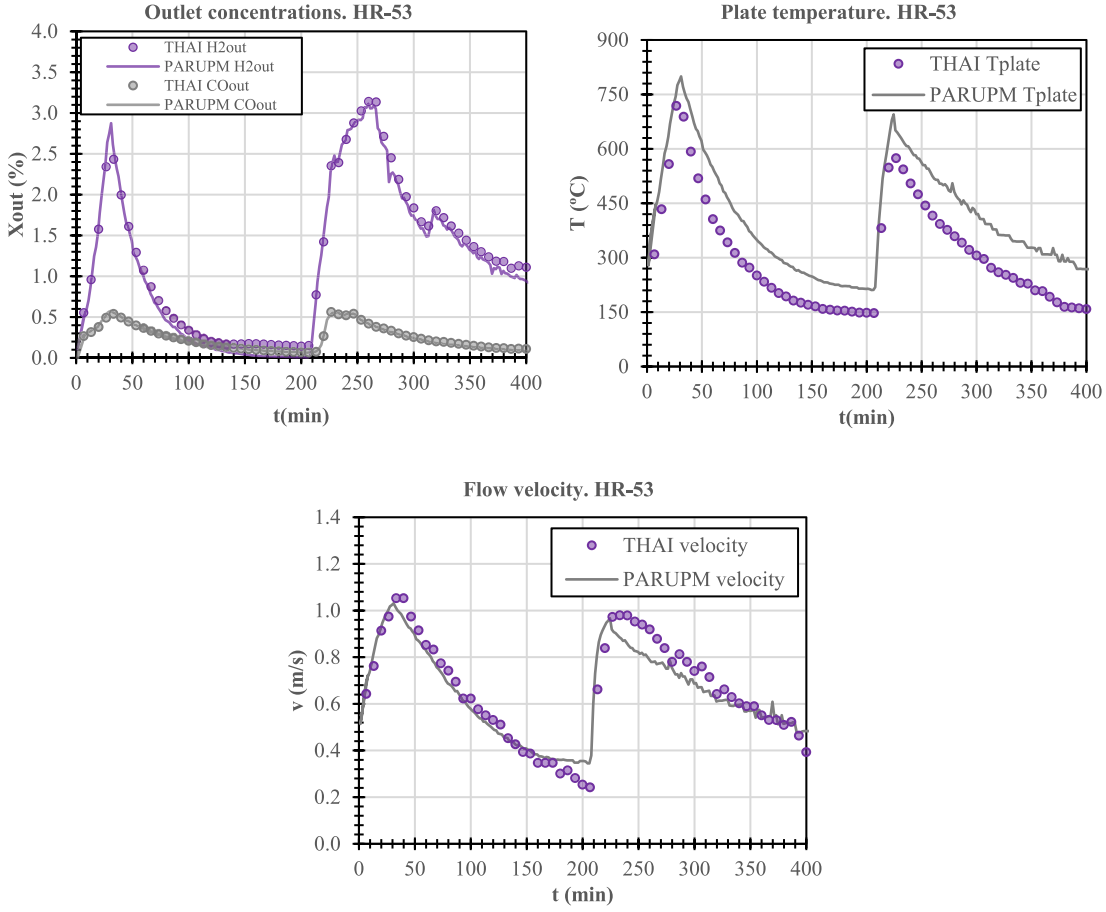

Fig. 14. H_2 and CO concentrations at the outlet of the PAR, catalyst temperature, and flow velocity with PARUPM and the corresponding experimental values during the HR-53 transient in the THAI facility.

5. Conclusions

The primary objective of this work was to introduce the PARUPM code along with a validation process to ascertain its applicability as a standalone tool. To achieve this, an initial refinement and validation of the code under steady-state conditions were performed utilizing the available data from the REKO-3 facility. Subsequently, the second phase of the validation focused on assessing the code performance under transient conditions utilizing the THAI data, wherein flow characteristics vary for every successive time step.

The steady-state validation process of PARUPM, performed with data from the REKO-3 facility, shows that the code has been successfully adapted to simulate specific conditions, such as oxygen starvation, and the impact of carbon monoxide on the recombination process. From the comparison of the experimental data and the simulated results, we find that the code demonstrated good accuracy in predicting recombination rates under the conditions examined. Therefore, the code is capable of replicating the behaviour of PARs in achievable conditions during steady-state conditions.

Furthermore, the validation process was extended to transient conditions using data from the THAI facility. Specific tests (HR-2, HR-12, HR-51, and HR-53) were simulated, and the PARUPM results were compared with the PAR specific experimental data for outlet concentrations, catalyst temperatures, and inlet flow velocities. From this comparison the code was found robust in its results, capturing the behaviour of a realistic recombiner under realistic transient conditions. Moreover, a CO poisoning criterion was introduced in the PARUPM code, limiting the recombination rate when the oxygen concentration on the catalyst surface falls below a certain threshold and giving a chemical explanation to the CO poisoning effect.

Overall, despite some limitations related to heat transfer phenomena not considered in the model, the PARUPM code demonstrated its capability for simulating the behaviour of PARs in a wide range of scenarios, including steady-state and transient conditions, oxygen starvation, and CO poisoning. In conclusion, the validation process outlined in the paper provides confidence in the accuracy and reliability of the PARUPM code for simulating the operational behaviour of passive autocatalytic recombiners in severe accident conditions. The findings contribute to advancing the understanding and prediction capabilities crucial for managing combustion or explosion risks in nuclear reactor containment buildings.

Within the AMHYCO project, the PARUPM code has been proposed as an appropriate tool for assessing the performance of PARs in nuclear containments. The phenomenology observed in a severe accident can be examined in more detail once the PARUPM code is implemented in thermal–hydraulic analysis codes, such as GOTHIC (EPRI, 2018), a general-purpose integrated thermal–hydraulic software package for the design, licensing, safety, and operational analysis of nuclear power plant containment and system components. As a conclusion, the final PARUPM code could be coupled with GOTHIC for its use as a coupled code for simulating real recombiner performance in full containment studies under realistic sever accident conditions.

CRediT authorship contribution statement

Araceli Dominguez-Bugarin: Writing – original draft, Visualization, Software, Methodology, Investigation, Formal analysis, Data curation, Conceptualization. **Ernst-Arndt Reinecke:** Writing – review & editing, Validation, Methodology, Investigation, Formal analysis, Data curation. **Gonzalo Jiménez:** Writing – review & editing, Supervision, Project administration, Methodology, Funding acquisition, Formal analysis, Conceptualization. **Miguel Ángel Jiménez:** Writing – review & editing, Validation, Software, Methodology, Formal analysis. **Sanjeev Gupta:** Writing – review & editing, Validation.

Declaration of competing interest

The authors declare that they have no known competing financial interests or personal relationships that could have appeared to influence the work reported in this paper.

Acknowledgments

The HR-2 and HR-12 tests were conducted in the frame of the OECD/NEA THAI project (2007-2009). The financial support of the participating countries to the OECD/NEA THAI project is gratefully acknowledged. The PAR recombiner test series HR-51 to HR-53 was funded by the German Federal Ministry for Economic Affairs and Energy under grant number 1501547, on the basis of a decision by the German Bundestag. Furthermore, the AMHYCO project has received funding from the Euratom research and training programme 2019-2020 under Grant Agreement n°945057. The content of this paper reflects only the author's view. The European Commission is not responsible for any use that may be made of the information it contains. Finally, this work has received funding from the ENEN2plus mobility grant program. The content of this paper reflects only the author's view. The European Commission is not responsible for any use that may be made of the information it contains.

Data availability

The authors do not have permission to share data.

References

Arnould, F., 2003. State of the Art of Passive Autocatalytic Recombiner (PARSOAR).
Bachellerie, E., Arnould, F., Auglaire, M., de Boeck, B., Braillard, O., Eckardt, B., Ferroni, F., Moffett, R., 2003. Generic approach for designing and implementing a passive autocatalytic recombiner PAR-system in nuclear power plant containments. Nucl. Eng. Des. 221 (1–3). https://doi.org/10.1016/S0029-5493(02)00330-8.
Bentaib, A., Meynet, N., Bleyer, A., 2015. Overview on hydrogen risk research and development activities: methodology and open issues. Nucl. Eng. Technol. 47. https://doi.org/10.1016/j.net.2014.12.001.
Boehm, J., 2007. Modelling of procecces in catalytic recombiners, Report Forschungszentrums Jülich. Energy Technology 61. ISBN 978-3-89336-473-2.
Carcassi, M., Bazzicchi, A., 1997. Empirical correlations for PAR performances. Universitá Di Pisa, CONT-HYMI (97)-D007.
Coward, H.F., Jones, G.W., 1952. Limits of flammability of gases and vapors,. US Government Printing Office.
Deutschmann, O., Schmidt, R., Behrendt, F., Warnat, J., 1996. Numerical modeling of catalytic ignition, in: Symposium (International) on Combustion, doi: 10.1016/S0082-0784(96)80400-0.
Domínguez-Bugarín, A., Jiménez, M.-Á., Reinecke, E.-A., Jiménez, G., 2022. PARUPM: A simulation code for passive auto-catalytic recombiners. EPJ Nuclear Sci. Technol. 8. https://doi.org/10.1051/epjn/2022046.
Elenbaas, W., 1942. Heat dissipation of parallel plates by free convection. Physica 9 (1), 1–28. https://doi.org/10.1016/S0031-8914(42)90053-3.
ENSREG, 2012. 'Peer review report: Stress tests performed on European Nuclear Power Plants.', v12i – 2012 04 25.
EPRI, 2018. GOTHIC Thermal Hydraulic Analysis Package. Version 8.3(QA). EPRI, Palo Alto, CA.
Framatome, 2024. Passive Autocatalytic Recombiner - Combustible Gas Control System. https://www.framatome.com/solutions-portfolio/docs/default-source/default-document-library/product-sheets/a0642-p-ge-g-en-202405-par.pdf?sfvrsn=ec8cb920_0.
Freitag, M., von Laufenberg, B., Colombet, M., Klauck, M., 2020. Measurements of the impact of carbon monoxide on the performance of passive autocatalytic recombiners at containment-typical conditions in the THAI facility. Ann. Nucl. Energy 141, 107356. https://doi.org/10.1016/j.anucene.2020.107356.
Gupta, S., Poss, G., Sonnenkalb, M., 2016. OECD/NEA THAI program for containment safety research: main insights and perspectives. presented at the Eurosafe Forum 2016, Münich, Germany.
Gupta, S., Freitag, M., Poss, G., 2021. THAI experimental research on hydrogen risk and source term related safety systems. Front. Energy 15 (4), 887–915. https://doi.org/10.1007/s11708-021-0789-1.
IAEA, 2011. Mitigation of hydrogen hazards in severe accidents in nuclear power plants. Vienna, IAEA-TECDOC-1661.
Jiménez, M.Á., 2007. 'Recombinación del hidrógeno en dispositivos autocatalíticos pasivos y sus implicaciones en la seguridad de las centrales nucleares'. Available: http://oa.upm.es/718/.
Jiménez, G., Herranz, L., Bentaib, A., Chaumeix, N., Reinecke, E.-A., Loeffler, M., Bratfisch, C., Kljenak, I., Sevbo, O., Visser, D., 2022. 'AMHYCO project-Towards an

enhanced accident management of the H2/CO combustion risk. In: presented at the The 19th International Topical Meeting on Nuclear Reactor Thermal Hydraulics (NURETH-19), Brussels, Belgium, 2022.

Jiménez, M.A. Martin-Valdepeñas, J.M., Martin-Fuertes, F., Fernandez, 2007. A detailed chemistry model for transient hydrogen and carbon monoxide catalytic recombination on parallel flat Pt surfaces implemented in an integral code. Nucl. Eng. Des. 237(5) (2007), doi: 10.1016/j.nucengdes.2006.08.002.

Klauck, M., Reinecke, E.-A., Kelm, S., Meynet, N., Bentaïb, A., Allelein, H.-J., 2014. Passive auto-catalytic recombiners operation in the presence of hydrogen and carbon monoxide: experimental study and model development. Nucl. Eng. Des. 266, 137–147. https://doi.org/10.1016/j.nucengdes.2013.10.021.

Gupta, S., Poss, G., Freitag, M., Schmidt, E., Colombet, M., von Laufenberg, B., Kühnel, A., Langer, G., Funke, F., Langrock, G., 2019. Experimental investigations on fission-product retention and hydrogen mitigation for design-basis and severe accidents in the containment - THAI-VI Final report. Becker Technologies, Germany.

Klauck, M., Reinecke, E.-A., Allelein, H.-J., 2021. Effect of par deactivation by carbon monoxide in the late phase of a severe accident. Ann. Nucl. Energy 151, 107887. https://doi.org/10.1016/j.anucene.2020.107887.

Kanzleiter, T., 2009b. Hydrogen recombiner tests HR-6 to HR-13, HR-29 and HR-30: tests with steam, using an AREVA PAR. Becker Technologies GmbH, Eschborn, Germany, 1326-HR-QLR-2.

Kanzleiter, T., 2009a. 'Quick Look Report on Hydrogen Recombiner Tests HR-1 to HR-5, HR-27 and HR-28 (Tests without steam, using an Areva PAR)', Becker Technologies GmbH, Eschborn, Germany, 1501326-HR-QLR-1.

NEA, 2010. OECD/NEA THAI Project Hydrogen and Fission Product Issues Relevant for Containment Safety Assessment under Severe Accident Conditions', NEA/CSNI/R (2010)3.

NEA, 2014. 'Status Report on Hydrogen Management and Related Computer Codes', NEA/CSNI/R(2014)8.

Payot, F., Reinecke, E.-A., Morfin, F., Sabroux, J.C., Meynet, N., Bentaib, A., March, P., Zeyen, R., 2012. Understanding of the operation behaviour of a Passive Autocatalytic Recombiner (PAR) for hydrogen mitigation in realistic containment conditions during a severe Light Water nuclear Reactor (LWR) accident. Nucl. Eng. Des. 248. https://doi.org/10.1016/j.nucengdes.2012.03.042.

Reinecke, E.-A., Fontanet, J., Herranz, L.E., Liang, Z., Maas, L., Mazurok, O., Park, J.-S., Visser, D.C., Hupp, M., Gupta, S., 2022. PAR model development exercise in the framework of SAMHYCO-NET. Nucl. Eng. Des. 399, 112035. https://doi.org/10.1016/j.nucengdes.2022.112035.

Reinecke, E.-A., Tragsdorf, I.M., Gierling, K., 2004. Studies on innovative hydrogen recombiners as safety devices in the containments of light water reactors. Nucl. Eng. Des. 230 (1–3). https://doi.org/10.1016/j.nucengdes.2003.10.009.

Reinecke, E.-A., Kelm, S., Struth, S., Schwarz, U., Tragsdorf, I.M., 2007. Performance of catalytic recombiners for hydrogen mitigation in severe accidents under oxygen depletion conditions. In: presented at the ICONE-15, Japan, 2007.

Reinecke, E.-A., Bentaib, A., Kelm, S., Jahn, W., Meynet, N., Caroli, C., 2010. Open issues in the applicability of recombiner experiments and modelling to reactor simulations. Progr. Nucl. Energy 52(1), 2010, doi: 10.1016/j.pnucene.2009.09.010.

Reinecke, E.-A., 2023. Hydrogen and carbon monoxide mitigation in light water reactors. AMHYCO Workshop, Orleans, France.